Multi-frequency low-noise semiconductor laser sources enabling advancement of resonant fiber optic gyroscopes including performance over temperature

Émile Girard-Deschênes, François Costin, Simon Ayotte*, André Babin, Katherine Légaré, Bruno Labranche, Laurent Dusablon, Jean-Sébastien Pelletier-Rioux, Patrick Dufour, Sébastien Deschênes, Rodrigo Falci, Ghislain Bilodeau, Philippe Chrétien, Charles-André Davidson, Dominique D'amato, Mathieu Laplante, Robert Baribault
TeraXion, 2716 rue Einstein, Québec, Québec, Canada G1P 4S8

Marc Smiciklas, Lee Strandjord, Chellappan Narayanan, Robert Compton, and Glen Sanders
Honeywell International, 21111 N. 19th Avenue, Phoenix, AZ, USA

ABSTRACT

We present multi-frequency low-noise semiconductor laser sources for resonant fiber optic gyroscope (RFOG) interrogation that have enabled excellent gyro stability over temperature. Each laser source includes three distributed feedback semiconductor laser chips coupled with micro-lenses to multi-component silicon photonics (SiP) chips. A first laser, the master, is locked to the RFOG with a Pound-Drever-Hall loop. Two slave lasers are optically phase-locked to the master laser with electrical loop bandwidths of 100 MHz. The SiP chips perform beat note detection and several other functions, such as phase and intensity noise suppression. The lasers and SiP chips are packaged in an optical engine that is controlled by compact low noise electronics. The fiber pigtails are connected to the RFOG so that light is sent in clockwise and counterclockwise directions. Tracking of the RFOG resonance frequencies in both directions allows rotation sensing. An ultra-stable differential frequency noise floor of 0.05 Hz/rt-Hz was obtained between the lasers and the coil resonator which was instrumental in achieving results for the RFOG over 60˚ C operating temperature range. The corresponding angle random walk level is less than 0.01 ˚/rt-hr and was not limited by laser differential frequency noise. The gyroscope bias drift over the tested temperature range was maintained within 0.005 ˚/hr, the best-ever published RFOG performance over temperature to date.

Keywords: Narrow linewidth semiconductor laser, resonant fiber optic gyroscope, silicon photonics, optical phase-locked, Pound-Drever-Hall method.

1. INTRODUCTION

The Resonator Fiber Optic Gyroscope (RFOG) measures rotation rate by comparing optically resonant frequency shifts between the clockwise (CW) and counterclockwise (CCW) directions in a multi-turn passive fiber ring resonator [1]-[2]. Despite its less proven performance, RFOG development, including at Honeywell, has been motivated by its potential to achieve better signal-to-noise performance for rotational sensing than Ring Laser Gyros (RLGs) and Interferometric Fiber Optic Gyros (IFOGs) for a given size [3]. This theoretical advantage is because the RFOG combines the signal-to-noise sensitivity attributes of both RLGs and IFOGs, given that light is circulated around the loop many times with increasing finesse (F), and multi-turn coils can be deployed to increase path length well beyond that in an RLG. Hence, RFOG development is motivated by the promise of an inexpensive, compact optical gyro for commercial navigation applications.

In an RFOG, the achievable sensitivity is proportional to the narrowness of the interferometric spectral feature interacting with the sensing light. Monitoring the shift of a narrow spectral feature under the action of a measurand requires a narrow linewidth optical source and high-quality control electronics. Furthermore, the monitoring of rapidly evolving phenomena requires electronics with sufficient bandwidth for tracking. A Pound-Drever-Hall (PDH) locking loop can achieve both objectives, i.e., tracking a narrow spectral feature with a bandwidth in the MHz range [4]. RFOG requires tracking the frequency difference between two narrow-spectral features (CW and CCW) [5]-[10]. Such differential sensing requires controlling the frequency difference between two lasers precisely. An optical phase-locked loop (OPLL) locks in phase two laser signals at a fixed or tunable frequency offset. In this paper we demonstrate optical sources having low noise lasers and high bandwidth locking electronics loops which are essential to demonstrate good angular random walk (ARW) gyroscope performance.

*sayotte@teraxion.com; phone 1-418-658-9500 ext. 482

Besides ARW, another crucial figure of merit of any gyroscope is bias drift. In RFOGs, a highly coherent source is required, so optical backscatter is a major challenge. Light backscatters from one wave into another and interferes with signal light. When the CW and CCW lightwaves, at frequencies f_{CW} and f_{CCW}, are near zero difference, $\Delta f=f_{CW}-f_{CCW}\sim 0$, bias errors result. Use of a multi-laser system with phase lock loops enables locking of CW and CCW waves to separate longitudinal lines of the resonator [6], thereby eliminating the possibility of f_{CW} and f_{CCW}, being near zero difference. We present a modulation technique [10] that reduces errors due to backscatter, illustrating its ability to reduce the drift due to optical backscatter while retaining a common modulation for CW and CCW resonance detection. The common modulation was first proposed in connection with reducing errors due to modulation imperfections that might otherwise affect bias instability if different modulation waveforms and frequencies were used for CW and CCW resonance detection. Bias stability results are based on these modulation techniques.

We present progress towards compact RFOGs using phase locked diode lasers and miniaturized optics on a silicon optical bench (SiOB). Further integration was realized by encapsulating unpackaged semiconductor lasers on a common substrate with a silicon photonics (SiP) chip comprising active and passive components [11]-[13]. Other than a reduction in size, this allowed a sizable increase in the bandwidth of the OPLL loops by shortening optical and electrical paths. The SiP chip carried more functionalities such as the PDH modulation of the master laser, power monitoring and variable optical attenuation for control of the optical output power.

2. MULTI-FREQUENCY LASER SOURCE

2.1 Architecture

The high-level schematic of the multi-frequency laser source (MFLS) is shown in Figure 1 and consists of all the optical components before the two optical circulators (see [13] for detailed architecture including SiP chip). The optical power at 1550 nm is provided by three distributed feedback (DFB) semiconductor lasers, a master laser and two slave lasers, developed by TeraXion in collaboration with the National Research Council of Canada (NRC). These lasers display a low frequency noise with an intrinsic linewidth of 10 kHz. Furthermore, they provide a nearly flat frequency modulation (FM) response up to frequencies greater than 100 MHz allowing an efficient frequency noise reduction by means of electronic feedback.

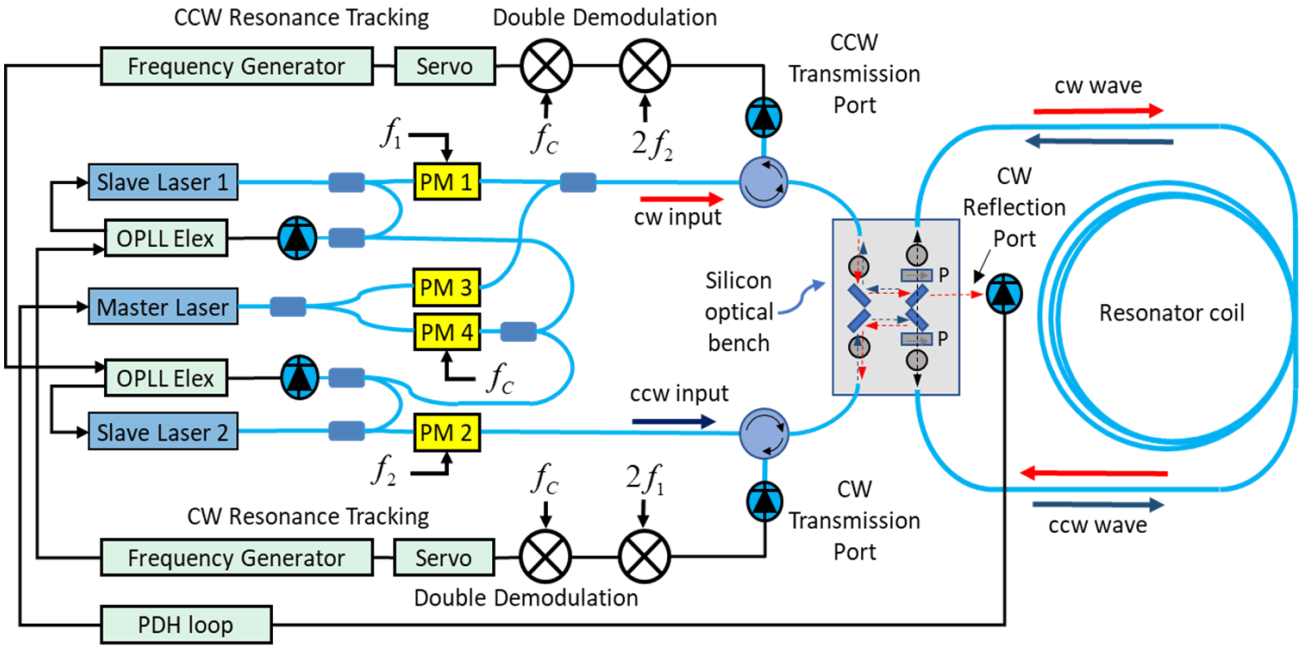

Figure 1 : High-level schematic of the complete RFOG. The multi-frequency laser source includes all the components that precede the two optical circulators.

Locking a laser to a passive optical resonator can reduce this frequency noise markedly. In the present instance, the master laser is locked to the side of the reflectivity spectrum of a narrow band (340 MHz) fiber Bragg grating (FBG) used as a frequency discriminator. The result is a reduction of laser noise by as much as 30 dB at frequencies up to 100 MHz (see orange trace on Figure 2). In addition, the master laser is locked to the resonator coil using the well-known Pound-Drever-Hall (PDH) stabilization technique. This is accomplished by directing a portion of the master laser light through a phase modulator (PM3 on Figure 1) where it is modulated to provide a PDH signal at the resonator CW reflection port which is demodulated by the PDH loop electronics. This PDH loop also acts on the master laser current to reduce relative noise between the lasers and the resonator below 100 kHz (see purple trace on Figure 2).

Another portion of the master laser light is directed through a phase modulator (PM4) and then optically mixed on photodiodes with portions of the slave laser light to generate beat notes. This is used by the optical phase-locked loop (OPLL) electronics to phase lock the slave laser frequencies to the master laser frequency plus offset frequencies produced by frequency generators. Each loop is acting on its respective slave laser injection current to reduce differential noise between the master laser and the slave laser at Fourier frequencies up to 25 MHz (see yellow trace on Figure 2). The slave lasers then share a common frequency noise equal to that of the master laser over a bandwidth limited by the OPLL bandwidth.

In a RFOG used for inertial sensing, rotation creates a differentiation of the resonance peaks for light propagating clockwise and counterclockwise within the optical fiber loop. The two slave lasers frequencies are tuned independently by their OPLL frequency generators to track resonance peak in CW and CCW and achieve rotation sensing. High sensitivity sensing is afforded when both slave lasers carry the same frequency noise, which then generates common mode noise that can be subtracted.

This high-performance source is compact, automated, robust, and remains locked for days. DFB and SiP on common submount allows small size factor which in turn allow high bandwidth electronics required for loops.

2.2 Feedback loop performance

Figure 2 presents measurements of power spectral densities of frequency noise (PSDFN) performed on the laser source. The intrinsic frequency noise of Teraxion's DFB lasers is as low as 3000 Hz2/Hz at high frequencies (blue trace) corresponding to a Lorentzian linewidth of 10 kHz. Locking the master laser to the FBG frequency discriminator reduces

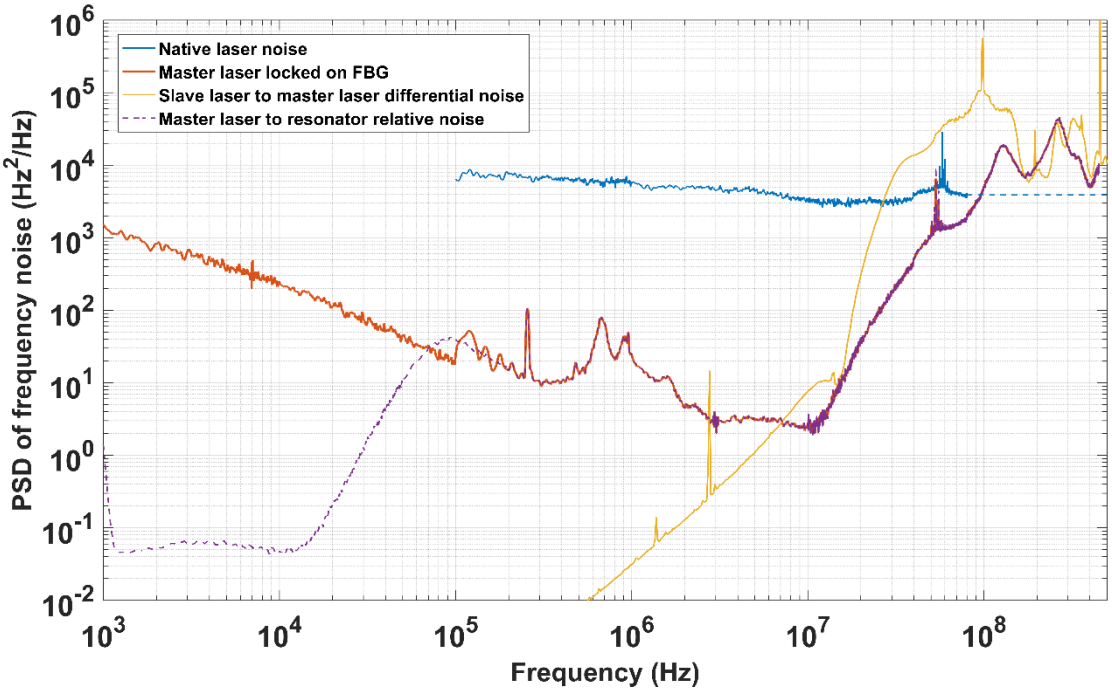

Figure 2 : Measured PSD of frequency noise of the multi-frequency laser source.

the frequency noise markedly, up to frequencies of 100 MHz (orange curve). The PDH loop further reduces the ML to resonator relative noise up to 100 kHz (purple trace). The yellow curve on the graph also highlights the successful subtraction of the frequency noises of the master laser and a slave laser resulting from their phase locking with an OPLL with loop bandwidths greater than 10s MHz. The PSDFN of the beat signal between the master laser and the second slave laser generated within the SiP chip stands at 0.03 Hz^2/Hz at 1 MHz, i.e., 52 dB below the intrinsic frequency noise level observed on the free running lasers.

The laser source has been tested for an operating temperature range between -10°C to +70°C and the loop performance from Figure 2 is stable. Optical power coming out of slave 1 and slave 2, after the SiP chip and into the fiber varies by less than 4% peak to peak for the whole range.

3. RFOG OPERATION WITH NOVEL MODULATION METHOD

The RFOG configuration with the modulation method presented in [10] is shown schematically in Figure 1. The sensing coil consists of a 100 m of polarization maintaining fiber wound on a two-inch diameter mandrel and a silicon optical bench (SiOB) holding tiny ball lenses, mirrors, and beam-splitters to close the resonator loop as well as provide light coupling into and out of the loop.

The phase modulation imposed by PM4 is transferred to the slave lasers as the common frequency modulation which is used for precise detection of the center frequencies of the CW and CCW resonance transmission peaks. This common modulation is applied at frequency f_C, which is relatively low compared to the resonator linewidth. The CW and CCW slave laser light pick up extra phase modulation by phase modulators PM1 and PM2 at frequencies f_1 and f_2 close to $(n+1/2) \times FSR$, where n is some integer. To suppress backscatter errors, CW and CCW high frequency (HF) modulation frequencies, f_1 and f_2, are set slightly different. When the laser carrier is exactly in the middle of two adjacent resonances, the first-order upper and lower sidebands produced by the HF modulation will be at the center frequency of the corresponding upper and lower transmission peaks. The two sidebands will interfere in the transmission port, thus producing a beat note that is at twice the HF modulation frequency. The common modulation, fc, can be viewed as sweeping the sidebands over the resonance peaks. Double demodulating the resonator transmission output at $2f_1$ and then at f_C will produce an error signal that indicates when the sidebands are exactly on resonance. The output of the second demodulator on Figure 1 is used as a feedback loop error signal to control the laser frequency to follow the resonator's resonance frequencies with a fixed offset. This double demodulation strategy mitigates the effects of Rayleigh backscattering.

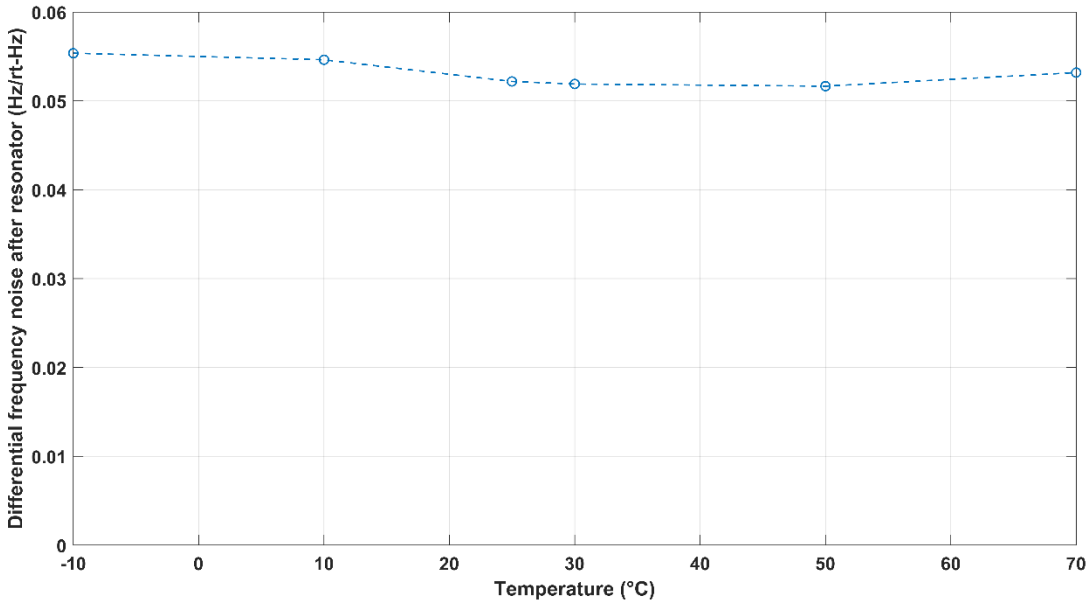

Figure 3 : Measured differential frequency noise (DFN) between CW and CCW signals as laser system temperature is increased.

Single laser frequency noise relative to the resonator is measured at each of the transmission ports of the high-finesse external resonator. *T*he lasers are locked on *the resonator* using fast photodiodes, low-noise transimpedance amplifiers and analog to digital converters to acquire noise in the time domain. Both time domain noise vectors are then subtracted to obtain differential frequency noise, on which a Fourier transform is made. The resulting white noise component of this transform is labeled differential frequency noise (DFN) and is reported in Figure 3 as a function of operation temperature. Its level varies slightly between 0.052 to 0.055 Hz/rt-Hz.

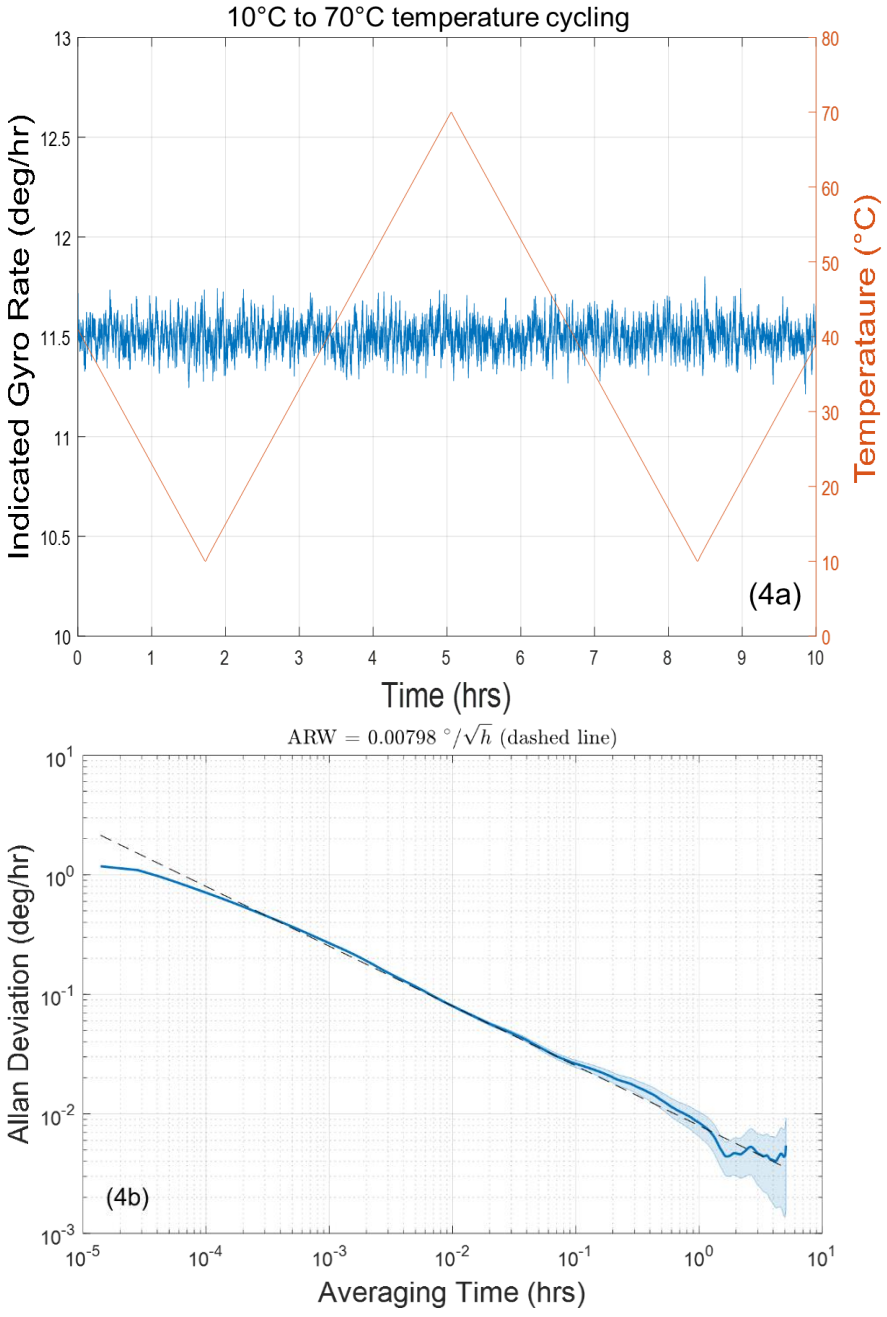

Figure 4a and 4b: Measured performance over temperature in RFOG. Figure 4a shows the compensated output of the gyro vs time as the temperature is ramped over a 60 ºC range. Figure 4b is an Allan Deviation plot of high-speed data taken from the gyro output while being temperature cycled as shown in 4a. It shows the ARW is 0.00798 deg/rt-hr and the bias stability, or long-term rotation uncertainty, is 0.005 deg/hr.

One can convert the DFN-only contribution to *ARW* with the following equation, where *n* is the index of refraction of the fiber coil and *D* is its diameter, keeping in mind that that gyro typically has other sources of noise:

$$ARW = DFN \times \frac{n \times 1550\,nm}{D} \times \frac{180}{\pi} \times \frac{3600}{60 * sqrt(2)}$$

To ascertain the performance of the gyro using the laser system, the gyro (except electronics) was subjected to temperature cycling from 10 ºC to 70 ºC. The laser system and gyro optics were found to perform very repeatably from temperature cycle to the next. Following a relatively standard procedure, a reference run was used to simulate factory calibration and to ascertain temperature coefficients of the gyro. The gyro output was then measured for a new temperature run and compensated with previously derived compensation coefficients. The gyro output versus time is plotted in blue in Figure 4a with the rotation rate scale on the left. The temperature is plotted versus time in orange with the scale on the right. The plot shows remarkably low temperature dependence and long-term drift.

To quantify the bias repeatability performance of the gyro, the compensated data was processed using a standard root Allan Variance technique, as shown in Figure 4b. As is shown in the figure, the rotation rate uncertainty for most integration times follows a negative ½ slope, indicating the that it is limited by white noise, or angle random walk. The minus 1/2 slope dashed line is indicative of the ARW, which is 0.00798 deg/rt-hr, over temperature. The bottom of the curve for long integration times, is a measure of bias instability. The bias instability is approximately 0.005 deg/hr during temperature cycling. This performance data represents widest reported temperature-test range for an RFOG, and the best performance over temperature to our knowledge.

4. CONCLUSION

A compact three-laser source with low frequency noise levels is used in combination with an RFOG. The excellent DFN performance demonstrated in a small mechanical form factor gives unique benefits to RFOGs. A new generation of MFLS is under development with improvements on the key MFLS metrics, focussing on further improving DFN, lowering the electrical power consumption, weight, and size. A major improvement on the DFN will come from increasing the laser optical power, reducing optical losses, and improving the component-to-component coupling. Increasing laser optical power comes from newly patented laser designs under development (160 mW, increase of factor 2), with native low-PSDFN. Low PSDFN decreases the constraints on the locking loops and contribute to the available optical power to the RFOG. Also in the works is a new generation of SiP chips, with optimized optical paths and coupling ratios with expected loss gain of about 1.5 dB. The overall optical power increase from the MFLS is expected to exceed 5 dB.

A novel modulation technique is also used to mitigate Rayleigh backscattering effects that affect bias drift in RFOGs. This technique imparts a frequency modulation at HF related to the resonator free spectral range on each of the counter-propagating waves, and one at low frequency. The HF modulation is slightly different for the two waves which suppresses intensity-type backscatter errors by at least two to three orders of magnitude. The low frequency modulation is used for precise resonance detection and is chosen to be common to the two lightwaves; thus, cancelling potential bias drift due to modulation imperfections.

The combination of exemplary laser system performance and careful gyro architecture design has resulted in the best RFOG performance over temperature that has been reported to our knowledge. Resulting long-term gyro bias drift was shown to be 0.005˚/hr over a 60 ºC temperature range, and the ARW was less that 0.008 deg/rt-hr. The differential frequency noise of the light source system was reduced to the point where it was not limiting gyro performance, and therefore, a very significant achievement. This is a major step towards the realization of a practical RFOG and is closing in on civil navigation grade performance.

ACKNOWLEDGEMENTS

TeraXion and Honeywell wish to thank the National Research Council of Canada (NRC) and the NRC's Canadian Photonics Fabrication Centre (CPFC) for their technical contribution to this work. TeraXion acknowledges the financial support provided by Honeywell International, the NRC's *Industrial Research Assistance Program*, and the Government of Quebec through the *SA²GE Greener Aircraft Mobilization Project*.

REFERENCES

[1] Ezekiel, S. and Balsam, S., "Passive ring resonator laser gyroscope, " Appl. Phys. Lett. 30(9), 478-480 (1977).

[2] Shupe, D., "Fiber resonator gyroscope: sensitivity and thermal non-reciprocity, " Appl. Opt. 20(2), 286-289 (1981).

[3] Ezekiel, S. and Arditty, H., "Fiber-optic rotation sensors," in [Fiber-Optic Rotation Sensors and Related Technologies], Springer-Verlag, Berlin & Heidelberg, 2-26, (1982).

[4] Drever, R. W. P., Hall, J. L. et al., "Laser phase and frequency stabilization using an optical resonator," Appl. Phys. B: Lasers Opt. **31**, 97-105 (1983).

[5] Tiequn Qiu, et al., "Performance of resonator fiber optic gyroscope using external-cavity laser stabilization and optical filtering", Proc. of the 23rd Intl. Conference on Fiber Optic Sensors, (2014).

[6] Wu, J. et al., "Resonator fiber optic gyro with high backscatter-error suppression using two independent phase-locked lasers," Proc. SPIE **9634**, 96341O (2015).

[7] Sanders, G. A. et al., "Fiber optic gyro development at Honeywell," Proc. SPIE **9852**, 985207 (2016).

[8] Smiciklas, M. et al., "Development and Evaluation of a Navigation Grade Resonator Fiber Optic Gyroscope," Joint Navigation Conference (2017).

[9] Sanders, G. A. et al., "Development of compact resonator fiber optic gyroscopes," IEEE Int. Symposium on Inertial Sensors and Systems (2017).

[10] L. K. Strandjord, et al., "Improved Bias Performance in Resonator Fiber Optic Gyros using a Novel Modulation Method for Error Suppression," in 26th International Conference on Optical Fiber Sensors, OSA Technical Digest (Optica Publishing Group, 2018), paper ThD3.

[11] Ayotte, S. et al., "Silicon Photonics-Based Laser System for High Performance Fiber Sensing," Proc. SPIE **9634**, 963413 (2015).

[12] Ayotte, S. et al., "Compact silicon photonics-based multi laser module for sensing," Proc. SPIE **10537**, 1053717 (2018).

[13] Ayotte, S. et al., " Compact silicon photonics-based laser modules for FM-CW LIDAR and RFOG," Proc. SPIE **11284**, 1128421 (2020).'